# Self-adaptation of chimera states

Nan Yao, Zi-Gang Huang, Hai-Peng Ren, Celso Grebogi, and Ying-Cheng Lai

Phys. Rev. E **99**, 010201 — Published 9 January 2019

DOI: 10.1103/PhysRevE.99.010201

# Self adaptation of chimera states

Nan Yao,[1] Zi-Gang Huang,[2,*] Hai-Peng Ren,[3] Celso Grebogi,[4] and Ying-Cheng Lai[5,6]

[1]*Department of Applied Physics, Xi'an University of Technology, Xi'an 710054, China*
[2]*School of Life Science and Technology, Xi'an Jiao Tong University, Xi'an 710049 China.*
[3]*Shaanxi Key Laboratory of Complex System Control and Intelligent Information Processing, Xi'an University of Technology*
[4]*Institute for Complex Systems and Mathematical Biology, King's College, University of Aberdeen, Aberdeen AB24 3UE, United Kingdom*
[5]*School of Electrical, Computer and Energy Engineering, Arizona State University, Tempe, AZ 85287, USA*
[6]*Department of Physics, Arizona State University, Tempe, Arizona 85287, USA*

(Dated: December 12, 2018)

Chimera states in spatiotemporal dynamical systems have been investigated in physical, chemical, and biological systems, and have been shown to be robust against random perturbations. How do chimera states achieve their robustness? We uncover a self-adaptation behavior by which, upon a spatially localized perturbation, the coherent component of the chimera state spontaneously drifts to an optimal location as far away from the perturbation as possible, exposing only its incoherent component to the perturbation to minimize the disturbance. A systematic numerical analysis of the evolution of the spatiotemporal pattern of the chimera state towards the optimal stable state reveals an exponential relaxation process independent of the spatial location of the perturbation, implying that its effects can be modeled as restoring and damping forces in a mechanical system and enabling the articulation of a phenomenological model. Not only is the model able to reproduce the numerical results, it can also predict the trajectory of drifting. Our finding is striking as it reveals that, inherently, chimera states possess a kind of "intelligence" in achieving robustness through self adaptation. The behavior can be exploited for controlled generation of chimera states with their coherent component placed in any desired spatial region of the system.

In spatially extended nonlinear dynamical systems, spontaneous symmetry breaking is common. For example, in a system of nonlocally coupled, identical nonlinear oscillators, coexistence of coherence and incoherence in distinct spatial regions can emerge during the spatiotemporal evolution of the system. This remarkable phenomenon was first observed about three decades ago in a numerical study of a system of coupled nonlinear Duffing oscillators [1], and was termed as "domain-like spatial structure." Later, the phenomenon was rediscovered [2], analyzed and given the name of "chimera" [3, 4]. Since then, there has been a great deal of interest in the subject [5**?** –57]. Chimera states have been studied in different types of systems such as regular networks of phase-coupled oscillators with a ring topology [2, 3, 5], regular networks hosting a few populations [6, 11], two-dimensional [4, 12] and three-dimensional lattices [38], torus [17, 29], and systems with a spherical topology [39]. Issues that were addressed include transient behaviors associated with chimera states [13–15], the effects of time delay [7, 10, 35], phase lags [18], coupling functions [22–24], and the impacts of random perturbation and complex topology of coupling [19, 25, 33, 37]. Experimentally, chimera states have been observed in a system of chemical oscillators [20, 26, 43], in an optical system [21, 45], in coupled mechanical oscillators [27], in electrochemical systems [28, 32], and even in quantum systems [44, 57]. Natural phenomena associated with chimera states include unihemispheric sleep [58, 59], neural spikes [60, 61], and possibly ventricular fibrillations [62]. Control of chimera states has also been investigated [31, 41, 46, 47, 56].

An issue of both theoretical and experimental interest is the robustness of the chimera states against external perturbations. In this regard, the effects of random removal of links were studied [25] with the finding that, even when a large number of links are removed so that chimera states are deemed not possible, in the state space there are still both coherent and incoherent regions, and the regime of conventional chimera state is a particular case in which the oscillators in the coherent region happen to be synchronized or phase-locked. Another work on networks of FitzHugh-Nagumo oscillators demonstrated that the chimera states are robust against irregular structural perturbations [63]. Quite recently, the robustness of chimera states in nonlocally coupled networks of nonidentical logistic maps was investigated [54]. These studies indicate that chimera states are generally robust against various kinds of external perturbations. The question is how does a chimera state respond to perturbation to achieve its robustness. Specifically, suppose the coherent component of the chimera state is disturbed so that the component is no longer coherent. If the state is to survive, it must adjust the relative distribution of the coherent and incoherent components in the space. That is, upon perturbation, a chimera state must reorganize itself into a new state, possibly through self adaptation, to generate a modified distribution of the coherent and incoherent components. How does the system accomplish this feat?

* huangzg@xjtu.edu.cn

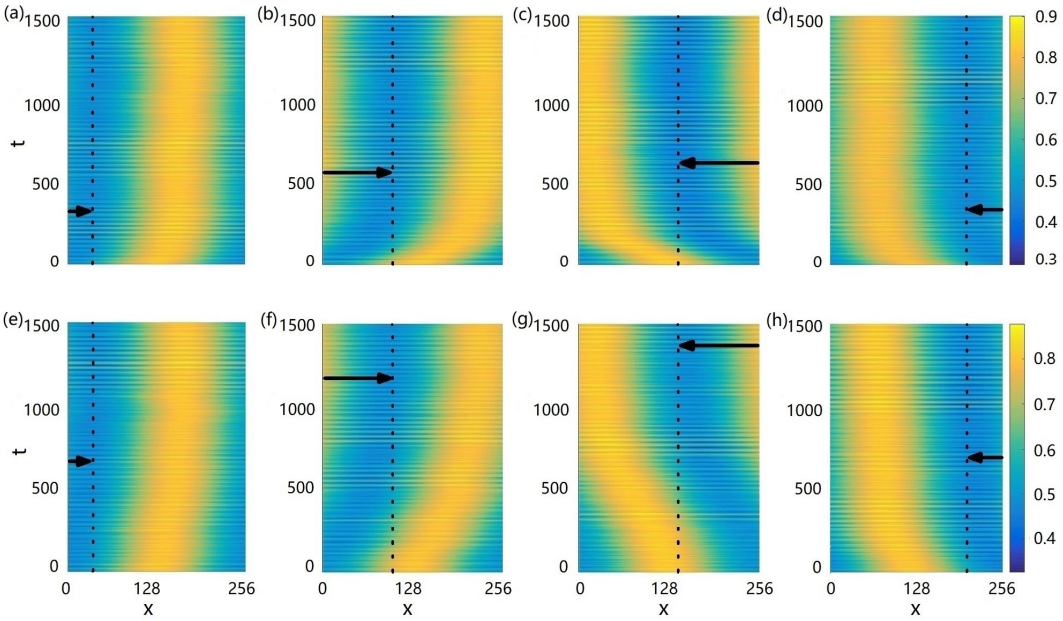


FIG. 1. (Color online) Self-adaptive, "intelligent" drift of chimera state in response to a spatially localized perturbation. The coherent and incoherent regions are represented by the yellow and blue colors, respectively. The drift is activated by disturbing a single node at the location $x_0$, where the perturbation strength is $\Delta\phi = 0.9\pi$ for the upper panels (a-d) and $0.3\pi$ for the lower panels (e-h). In each panel, the black arrow indicates the direction of drifting of the chimera state and the arrow length represents the drifted distance. The vertical location of the arrow specifies the time when the drifting chimera state settles down (or becomes stable). Other parameters are $A = 0.995$, $\alpha = 1.39$, and $N = 256$ (system size).

In this paper, we report a remarkable phenomenon of self adaptation of chimera states. When a spatially localized external perturbation is applied to the coherent component of a chimera state, it initiates and executes a self-adaptive drifting process toward an optimal state in which the incoherent component masks the perturbation and the newly formed coherent component is as far away as possible from the perturbation site. The response of the system is then to evolve toward a new chimera state that shields itself from the perturbation in an optimal way. Not only that, the system is also capable of selecting the optimal path towards the new chimera state. Carrying out a detailed analysis of the collective dynamics and patterns associated with the spatiotemporal evolution of the chimera, we identify the essential physical ingredients associated with the self-adaption process: an exponential relaxation of the chimera state toward the new stable state and the collapse of the relaxation trajectories into a single one independent of the location of perturbation. These behaviors enable us to construct a phenomenological model for a physical understanding of self adaptation of the chimera states. Taken together, the response of a chimera state to a perturbation through self adaptation is indicative of some intrinsic "intelligence" of the state, which not only is theoretically interesting, but also has implications to control or manipulation of chimera states in experimental systems.

We consider the paradigmatic setting for studying chimera states [2, 3, 5]: a ring network of $N$ non-locally coupled, identical phase oscillators with the periodic boundary condition: $d\phi(x_i)/dt = \omega - (2\pi/N)\sum_{j=1}^{N} G(x_i, x_j)\sin[\phi(x_i) - \phi(x_j) + \alpha]$, where $\phi(x_i)$ is the phase of the $i$th oscillator at spatial location $x_i$ and the range of the spatial variable is $[-\pi, \pi]$. The angular velocity $\omega$ and phase lag $\alpha$ of the oscillators are constants in space. Without loss of generality, we set $\omega = 0$ and $\alpha \lesssim \pi/2$. The kernel $G(x_i, x_j) = [1 + A\cos(x_i - x_j)]/(2\pi)$ is a non-negative even function that defines the non-local coupling among all the oscillators. For the ring system, chimera states are common [2, 3, 5], as exemplified in Fig. 1.

We numerically solve the system of coupled phase oscillators using the standard fourth-order Runge-Kutta integration method. To assess how perturbations affect the chimera state, we disturb the dynamical variable of a single oscillator (the target oscillator) at location $x_0$ that belongs to the coherent component. The nature of the perturbation is to force upon the oscillator a constant phase difference $\Delta\phi$ with respect to the local mean phase $\bar{\phi}_{\rm local}$ of its $2z$ neighbors, with equal number of neighbors on the left and right sides. Because of the perturbation, the originally coherent component is no longer coherent, and the chimera state, if it is to remain, must adjust itself to a new stable state. How does this occur?

Figure 1 shows the spatiotemporal pattern of the chimera state in response to perturbation of two strength values at different locations. Instead of evolving into a globally coherent or incoherent state, the original state maintains its chimerical character by shifting the coher-

ent component to a new region that is as far away as possible from the perturbed oscillator. At the same time, the incoherent component evolves to a region that contains the perturbed oscillator approximately at the center. This remarkable self adaptive behavior represents an "intelligent" scheme of the chimera state to protect itself.

Two characteristics of the spatiotemporal evolution of the chimera state in response to a perturbation are as follows. Firstly, after the perturbation is applied at $x_0$, the incoherent region begins to drift until its center $x_{\rm mid}(t)$ reaches $x_0$. This is surprising as, intuitively, one might expect the drift to stop once the incoherent region contains the location $x_0$. Each panel in Fig. 1 presents the relevant features: the midpoint $x_{\rm mid}(t)$ of the incoherent (blue) region, the target node at $x_0$, the corresponding time for $x_{\rm mid}(t)$ to reach $x_0$ (the vertical location $\tau$ of the arrow), and the instant when $x_0$ is just covered by the incoherent region (indicated by $t_{\rm cover}$ at which the coherent-incoherent boundary $x_{\rm bound}$ crosses $x_0$). We have $t_{\rm cover} < \tau$, indicating that the drift is not terminated even when the target node has already been covered by the incoherent region. The phenomenon is counterintuitive because the expectation is that, once the target node is merged in the incoherent region, the movement of the state should stop as the phases and the velocities of the individual oscillators in the incoherent region are nonetheless intrinsically random. The fact that the state continues to drift until $x_{\rm mid}$ reaches $x_0$ implies a kind of self adaptation among the oscillators toward an optimal state that makes the chimera state as robust as possible. Indeed, the drift terminates when $x_{\rm mid} = x_0$ so that the new chimera state possesses a global symmetry with maximum robustness. Because of the "desire" for the chimera state to acquire the symmetry, a perturbation even in the originally incoherent region, which breaks the global symmetry of the chimera state, would induce a drift. This has indeed been observed numerically. In fact, once the state has been stabilized, the order parameter $R(x)$ of the midpoint $x_{\rm mid}$ in the incoherent region reaches a minimum value, providing a way to calculate the value of $x_{\rm mid}$. Secondly, the system always chooses the shorter path for $x_{\rm mid}$ to drift toward $x_0$, as indicated by the length of the arrow in each panel of Fig. 1. Especially, because of the periodic boundary condition, there are two possible routes of drifting. For every case examined, the drift takes place along the shorter path.

To gain further insights into the physical mechanism of the self-adaptive behavior of chimera states, we examine the temporal dynamics of drifting. Specifically, for a given chimera state with its coherent region centered at $N/2$, we monitor the evolution of $\Delta x(t) \equiv |x_{\rm mid}(t) - x_0|$ for different values of $x_0$, as shown in Fig. 2(a) for $\Delta\phi = 0.3\pi$. In all cases, $\Delta x(t)$ converges to zero with small fluctuations introduced by intrinsic noise of the finite size system. The relaxation time $\tau$ of the self-adaptive drifting is effectively the first passage time of the smoothed $\Delta x(t)$ curve to zero. Figure 2(b) shows $\tau$ versus $x_0$ and $\Delta\phi$. We see that, when $x_0$ is closer to the

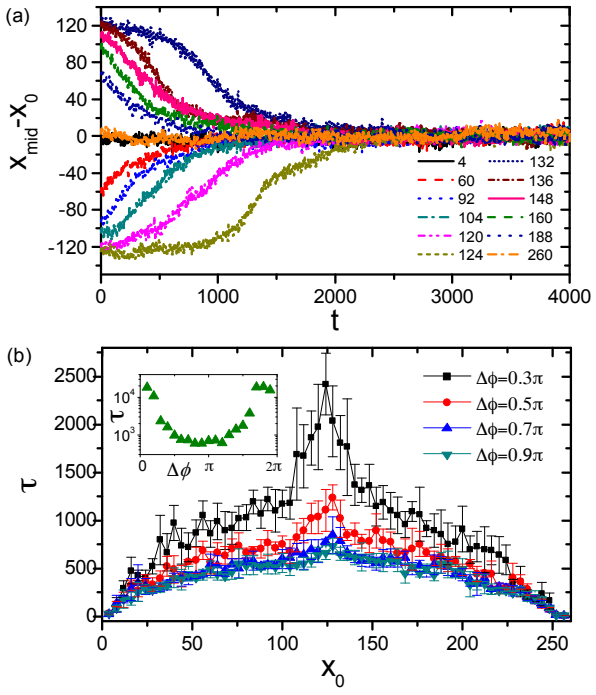


FIG. 2. (Color online) Spatial movement and relaxation time of chimera associated with self-adaptive drifting. (a) Distance between the middle point $x_{\rm mid}$ of the incoherent region of the chimera state and the location $x_0$ of the target oscillator. For different values of $x_0$, the chimera state drifts until $x_{\rm mid}(t)$ covers $x_0$, i.e., $x_{\rm mid}(t) - x_0$ converges to 0. (b) The relaxation time $\tau$ for the chimera state to become stable again versus $x_0$ and the perturbation strength $\Delta\phi$, respectively.

center of the coherent region ($x = N/2$), $x_{\rm mid}(t)$ travels a longer distance to reach $x_0$, leading to a larger value of $\tau$. The impact of the perturbation strength $\Delta\phi$ on the drifting process is symmetric about $\pi$ under the periodic boundary condition, as shown in the inset of Fig. 2(b). It can also be seen that, for small perturbation ($\Delta\phi \sim 0$ or $2\pi$), the drifting process slows down significantly with the relaxation time $\tau$ approximately one order of magnitude higher than that associated with $\Delta\phi \sim \pi$. In general, we find that the spatial pattern of a chimera state tends to be more robust in larger size systems with respect to different kinds of perturbation, facilitating the emergence of the self-adaptive drifting behavior. In fact, for a larger system, the parameter region for generating the drifting behavior is larger.

Does the self-adaptive drifting process have any memory of the value of $x_0$? The question can be addressed by examining whether two intermediate states evolving from different initial states and having the same value of $\Delta x(t)$ at some time $t$ can be distinguished. To facilitate a comparison, we use the transformed time $t' = t + t_0(x_0)$, where $t_0(x_0)$ is the time at which the dynamical variables of all the oscillators collapse to a single point. Any subsequent collapse would be indicative of lack of any memory effect. Figure 3(a) shows $|\Delta x(t')|$ for different

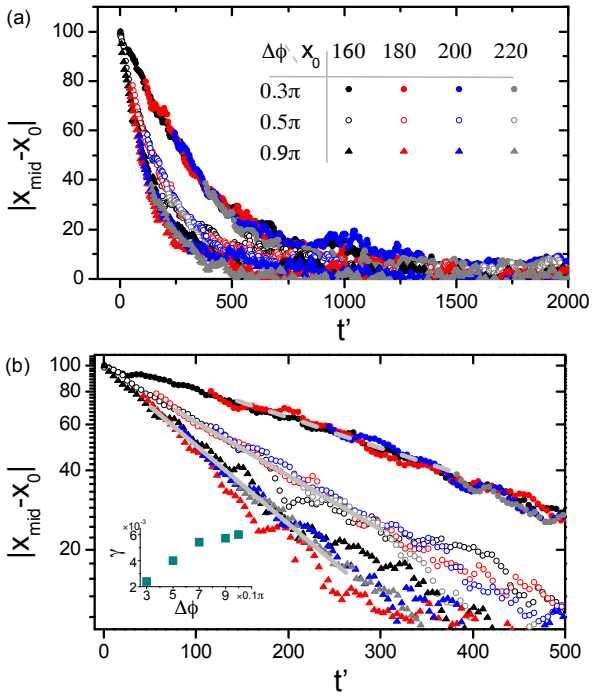


FIG. 3. (Color online) Collapse of drifting trajectories. (a) In the transformed coordinate $t'$, the absolute distances $|x_{\rm mid}(t') - x_0|$ resulting from different values of $x_0$ collapse into one, implying that the chimera state drifts according to the distance between $x_{\rm mid}(t)$ and $x_0$. (b) The same data on a logarithmic-normal plot, where the exponentially decaying behavior $|x_{\rm mid}(t') - x_0| \sim e^{-\gamma t}$ can be seen. The perturbation strength is $\Delta\phi = 0.3\pi$ (solid circles), $0.5\pi$ (open squares), and $0.9\pi$ (solid triangles). The value of the exponential rate $\gamma$ increases with $\Delta\phi$.

values of $x_0$. The three classes of collapsed curves correspond to different values of the perturbation strength $\Delta\phi$. Because of the collapses, any memory effect in the spatiotemporal evolution of the chimera state upon perturbation can be ruled out. Figure 3(b) shows the same data but on a logarithmic-normal plot, which indicates an exponential decay: $\Delta x(t) \sim e^{-\gamma t}$, with $\gamma$ being the rate of decay whose value increases with $\Delta\phi$. That is, a larger perturbation induces faster drifting of the chimera. A remarkable feature in Fig. 3 is that, for a given value of the perturbation strength $\Delta\phi$, all the trajectories collapse into one, indicating that the distance between $x_{\rm mid}(t)$ and $x_0$ is the sole factor determining the self-adaptive drifting process. The exponential decay of $\Delta x$ associated with self-adaptive drifting is general and robust with respect to parameter variations not only for single-headed chimera as shown in Fig. 1, but also for multi-headed chimera states [64].

To gain theoretical insights, we examine the effect of a particular type of perturbations: these applied to oscillators at the boundaries between the coherent and incoherent regions located at $x_{\rm bound}$, as the drifting process is essentially determined by the movement of the boundaries. Let $\eta = n_{\rm incoh}/N$ be the fraction of the incoherent region associated with an unperturbed chimera state, where the value of $\eta$ depends on parameters such as the coupling strength $A$ and the phase lag $\alpha$. When a perturbation is applied to the oscillator at the center of the incoherent region, the value of $\eta$ tends to increase slightly, somewhat pushing the boundary into the coherent region. However, analysis reveals that any small change in the value of $\eta$ tends to diminish, restoring the original ratio between the coherent and incoherent regions [5].

Based on the numerical results, we articulate a phenomenological model to account for the impact of perturbation on the chimera state. Figure 4 presents a schematic illustration of the dynamics of the boundaries between the coherent and incoherent regions, where the left and right boundaries are located at at $x_l$ and $x_r$, respectively. Let $f_l$ and $f_r$ be the effective forces induced by the perturbation at $x_0$ to push the left and right boundaries, respectively. The distance from $x_0$ to the left (right) boundary is $L_l$ ($L_r$), and the width of the incoherent region is $L = L_l + L_r$. The effective force $f_l$ ($f_r$) depends on $L_l$ ($L_r$). The mathematical forms of these forces can be derived from the dynamical behavior of $\Delta x(t)$. In particular, the exponential decay of $\Delta x(t)$ with time indicates that the velocity and acceleration of the drifting also decay exponentially with time at the same rate. We define $y \equiv |\Delta x(t)|\mathcal{A}e^{-\gamma t}$ to obtain $\dot{y} = -\gamma\mathcal{A}e^{-\gamma t} = -\gamma y$ and $\ddot{y} = \gamma^2\mathcal{A}e^{-\gamma t} = \gamma^2 y$. The effective force upon the chimera state can be written as $F = m\ddot{y} = m\gamma^2 y$.

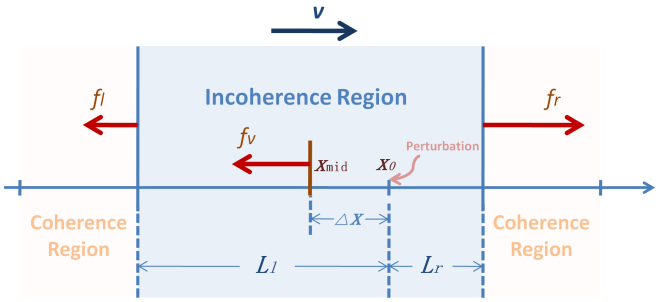


FIG. 4. (Color online) A schematic illustration of the effective, perturbation-induced forces in the phenomenological model. Perturbation at $x_0$ induces forces $f_l$ and $f_r$ on the left and right coherent-incoherent boundaries, respectively. The deceleration of the chimera state drifting towards the right-hand side indicates the existence of a damping force $f_v$. The periodic boundary condition has been taken into account in the distance calculation.

The linear dependence of the effective force $F$ on $y$ suggests that the force contain two components: a linear restoring force $F_k(y) = -ky$ and a damping force $f_v = -\eta\dot{y}$, with $k$ being the elastic constant and $\eta$ being the damping coefficient. The evolution of $y(t)$ obeys the equation: $m\ddot{y} + \eta\dot{y} + ky = 0$. From the function of $\ddot{y}$ and $\dot{y}$, we have $m\gamma^2 y - \eta\gamma y + ky = 0$, leading to the relation $k = \gamma(\eta - m\gamma)$ and hence the critical value of damping be-

yond which $y(t)$ decays exponentially to zero. The effect of perturbation on the chimera state can then be regarded as the result of the forces acting upon the two boundaries: $F_k(y) = f_r + f_l$. We have $F_k(y) = -\gamma(\eta - m\gamma)y$. Since $y = (L_l - L_r)/2$, we can also get the forces acting upon the left and right boundaries as $f_l = -\mathcal{B}\gamma^2(L_0 - L_l)/2$ and $f_r = \mathcal{B}\gamma^2(L_0 - L_r)/2$, respectively. The value of $L_0$ does not affect the movement of the chimera state. Because of the conservative nature of the restoring force, the minimum potential energy occurs at $y = 0$. The presence of the critical linear damping force $f_v$ leads to the exponential decay of $y(t)$ towards the minimum energy state. The phenomenological model thus explains the perturbation induced, self-adaptive drifting dynamics of the chimera state.

To further justify the phenomenological model, we resort to the two commonly used theoretical tools in the analysis of chimera states: the continuity equation [9] and the concept of invariant manifold [65, 66]. In general, the chimera dynamics can be characterized [2] by the following complex order parameter $Z$ defined for oscillator $i$ as $Z(x_i) \equiv R(x_i)e^{\mathrm{i}\Theta(x_i)} = (2\pi/N)\sum_{j=1}^{N} G(x_i - x_j)e^{\mathrm{i}\theta(x_j)}$, where the phase of the oscillator is $\theta = \phi - \Omega t$ with $\Omega$ being the phase velocity of the oscillators in the coherent subset when a chimera state emerges. Theoretical insights into the chimera states can be obtained by examining the continuum limit $N \to \infty$, where the system can be described by a one-dimensional PDE [65, 66]. In particular, the state of the system can be characterized by a probability density function $f(x, \phi, t)$ governed by the continuity equation $\partial f/\partial t + \partial/\partial\phi(f\mathrm{v}) = 0$, with v being the phase velocity [9]. The function $f(x, \phi, t)$ can be expressed in terms of Fourier series expansion as $f(x, \phi, t) = [1/(2\pi)]\{1 + \sum_{n=1}^{\infty}[h^n(x, t)e^{\mathrm{i}n\phi} + \mathrm{c.c.}]\}$, where "c.c." stands for the complex conjugate of the preceding term, and the $n$th coefficient is the $n$th power of some function $h(x, t)$ that effectively characterizes the state of the system. The time evolution of $h(x, t)$ associated with the order parameter $Z(x, t)$ is given by [65, 66] $\partial h(x, t)/\partial t = -\mathrm{i}\omega h(x, t) + \frac{1}{2}\left[Z^*(x, t)e^{\mathrm{i}\alpha} - Z(x, t)e^{-\mathrm{i}\alpha}h^2(x, t)\right]$, where $Z(x, t) = \int_{-\pi}^{\pi} G(x - x')h^*(x', t)dx'$ and $G(x - x')$ is the coupling function with normalized $x$: $G(x - x') = [1 + A\cos(x - x')]/(2\pi)$ for $-\pi < |x - x'| \le \pi$. Since the perturbation $\Delta\phi$ upon the phase of one single oscillator does not break the spacial pattern of the chimera but just induces the drifting of chimera as a whole, the theoretical description is applicable.

The impact of perturbation $\Delta\phi$ at $x_0$ can be characterized as $h(x_0) = h_0(x_0)e^{i\Delta\phi}$ or $h^*(x_0) = h_0^*(x_0)e^{-i\Delta\phi}$ based on the Fourier series expansion, with $h_0(x_0)$ and $h_0^*(x_0)$ denoting the respective values in the absence of perturbation. We then have $\delta h(x_0) = h_0(x_0)(e^{i\Delta\phi} - 1)$ and $\delta h^*(x_0) = h_0^*(x_0)(e^{-i\Delta\phi} - 1)$. From the evolutionary equation of $h(x, t)$, we have that the variances of $Z$ and $Z^*$ due to the perturbation at $x_0$ are $\delta Z = (2\pi/N)G(x - x_0)\delta h^*(x_0)$ and $\delta Z^* = (2\pi/N)G(x - x_0)\delta h(x_0)$, respectively. The variance of $\partial h/\partial t$ is $\delta\dot{h}(x, t) = -(1/2)e^{-i\alpha}h^2(x, t)\delta Z + (1/2)e^{i\alpha}\delta Z^* = (\pi/N)G(x - x_0)[\mathcal{X} - \mathcal{X}^*h^2(x, t)]$, with $\mathcal{X} = e^{i\alpha}\delta h(x_0)$. This provides a physical picture of how perturbation affects the chimera state. In particular, a larger value of the perturbation strength $\Delta\phi$ leads to a higher probability for a larger deviation $\delta\dot{h}(x, t)$ in the evolution, and the focal oscillator at $x$ with a smaller distance to $x_0$ gains a larger value of $\delta\dot{h}$ due to the larger value of $G(x - x_0)$. The deviation $\delta\dot{h}$ from the original chimera state reduces the stability of the coherent region and enlarges the incoherent region from the boundaries of the two regions at the speed $\delta\dot{h}(x, t)$. As shown in Fig. 4, a larger disturbance takes place at the oscillator closer to the boundary, i.e., the right-hand side boundary at $x_r$ (since $L_r < L_l$). Additionally, due to the intrinsic inertia of the chimera state to maintain the fraction between the coherent and incoherent regions, the expansion of incoherent region takes place at the right-hand side boundary.

To summarize, we uncover a striking phenomenon that occurs when a chimera state is disturbed: the state is capable of self-organizing into a new stable state in an adaptive and optimal way. Especially, when a spatially localized perturbation is applied to the coherent region, the chimera state is able to quickly "move" in the space (in an exponential fashion) to generate a new stable coherent region at the maximum distance from the perturbed oscillator through a path that is energy efficient. All these happen as if the chimera was "intelligent." We develop a simple mechanical model to account for these features, which is justified qualitatively by a theoretical analysis. It has been known that chimera states are robust. Our work provides a clear physical and dynamical picture on how the robustness is achieved. Experimental effort to verify the self-adaptive dynamics of chimera states uncovered in this paper will be appreciated.

This work was partially supported by the National Natural Science Foundation of China (Grant No. 11647052), by the Scientific Research Program Funded by Shaanxi Provincial Education Department (Program No. 17JK0553), by the Young Talent fund of University Association for Science and Technology in Shaanxi, China (Program No. 20170606), and by the Natural Science Basic Research Plan in Shaanxi Province of China (Program No. 2018JQ1010). ZGH acknowledges support of K. C. Wong Education Foundation. YCL is supported by ONR under Grant No. N00014-16-1-2828.

[1] D. K. Umberger, C. Grebogi, E. Ott, and B. Afeyan, Phys. Rev. A **39**, 4835 (1989).

[2] Y. Kuramoto and D. Battogtokh, Nonlinear Phenom. Complex Syst. **5**, 380 (2002).

[3] D. M. Abrams and S. H. Strogatz, Phys. Rev. Lett. **93**, 174102 (2004).
[4] S.-I. Shima and Y. Kuramoto, Phys. Rev. E **69**, 036213 (2004).
[5] D. M. Abrams and S. H. Strogatz, Int. J. Bifurcation Chaos **16**, 21 (2006).
[6] D. M. Abrams, R. Mirollo, S. H. Strogatz, and D. A. Wiley, Phys. Rev. Lett. **101**, 084103 (2008).
[7] G. C. Sethia, A. Sen, and F. M. Atay, Phys. Rev. Lett. **100**, 144102 (2008).
[8] C. R. Laing, Chaos **19**, 013113 (2009).
[9] C. R. Laing, Physica D **238**, 1569 (2009).
[10] J. H. Sheeba, V. K. Chandrasekar, and M. Lakshmanan, Phys. Rev. E **79**, 055203 (2009).
[11] E. A. Martens, Chaos **20**, 043122 (2010).
[12] E. A. Martens, C. R. Laing, and S. H. Strogatz, Phys. Rev. Lett. **104**, 044101 (2010).
[13] O. E. Omel'chenko, M. Wolfrum, and Y. L. Maistrenko, Phys. Rev. E **81**, 065201 (2010).
[14] M. Wolfrum and O. E. Omel'chenko, Phys. Rev. E **84**, 015201 (2011).
[15] M. Wolfrum, O. E. Omel'chenko, S. Yanchuk, and Y. L. Maistrenko, Chaos **21**, 013112 (2011).
[16] I. Omelchenko, Y. Maistrenko, P. Hövel, and E. Schöll, Phys. Rev. Lett. **106**, 234102 (2011).
[17] O. E. Omel'chenko, M. Wolfrum, S. Yanchuk, Y. L. Maistrenko, and O. Sudakov, Phys. Rev. E **85**, 036210 (2012).
[18] Y. Zhu, Y. Li, M. Zhang, and J. Yang, Europhys. Lett. **97**, 10009 (2012).
[19] C. R. Laing, K. Rajendran, and I. G. Kevrekidis, Chaos **22**, 013132 (2012).
[20] M. R. Tinsley, S. Nkomo, and K. Showalter, Nat. Phys. **8**, 662 (2012).
[21] A. M. Hagerstrom, T. E. Murphy, R. Roy, P. Hövel, I. Omelchenko, and E. Schöll, Nat. Phys. **8**, 658 (2012).
[22] I. Omelchenko, O.E. Omelchenko, P. Hövel, and E. Schöll, Phys. Rev. Lett. **110**, 224101 (2013).
[23] S. R. Ujjwal and R. Ramaswamy, Phys. Rev. E **88**, 032902 (2013).
[24] Y. Zhu, Z. Zheng, and J. Yang, Europhys. Lett. **103**, 10007 (2013).
[25] N. Yao, Z.-G. Huang, Y.-C. Lai, and Z.-G. Zheng, Sci. Rep. **3**, 3522 (2013).
[26] S. Nkomo, M. R. Tinsley, and K. Showalter, Phys. Rev. Lett. **110**, 244102 (2013).
[27] E. A. Martens, S. Thutupalli, A. Fourrière, and O. Hallatschek, Proc. Nat. Acad. Sci. (U.S.A) **110**, 10563 (2013).
[28] L. Larger, B. Penkovsky, and Y. Maistrenko, Phys. Rev. Lett. **111**, 054103 (2013).
[29] M. J. Panaggio and D. M. Abrams, Phys. Rev. Lett. **110**, 094102 (2013).
[30] C. Gu, G. St-Yves, and J. Davidsen, Phys. Rev. Lett. **111**, 134101 (2013).
[31] J. Sieber, O. E. Omel'chenko, and M. Wolfrum, Phys. Rev. Lett. **112**, 054102 (2014).
[32] L. Schmidt, K. Schönleber, K. Krischer, and V. García-Morales, Chaos **24**, 013102 (2014).
[33] Y. Zhu, Z. Zheng, and J. Yang, Phys. Rev. E **89**, 022914 (2014).
[34] O. E. Omel'chenko, Nonlinearity **26**, 2469 (2013).
[35] O. E. Omel'chenko, Y. L. Maistrenko, and P. A. Tass, Phys. Rev. Lett. **100**, 044105 (2008).
[36] J. Xie, E. Knobloch, and H.-C. Kao, Phys. Rev. E **90**, 022919 (2014).
[37] N. Yao, Z.-G. Huang, C. Grebogi, and Y.-C. Lai, Sci. Rep. **5**, 12988 (2015).
[38] Y. Maistrenko, O.Sudakov, O. Osiv, and V. Maistrenko, New J. Phys. **17**, 073037 (2015).
[39] M. J. Panaggio and D. M. Abrams, Phys. Rev. E. **91**, 022909 (2015).
[40] M. J. Panaggio and D. M. Abrams, Nonlinearity **28**, R67 (2015).
[41] E. A. Martens and C. Bick, New J. Phys. **17**, 033030 (2015).
[42] I. Omelchenko, A. Zakharova, P. Hövel, J. Siebert, and E. Schöll, Chaos **25**, 083104 (2015).
[43] S. Nkomo, M. R. Tinsley, and K. Showalter, Chaos **26**, 094826 (2016).
[44] D. Viennot and L. Aubourg, Phys. Lett. A **380**, 678 (2016).
[45] J. D. Hart, K. Bansal, T. E. Murphy, and R. Roy, Chaos **26**, 095801 (2016).
[46] L. V. Gambuzza and M. Frasca, Phys. Rev. E **94**, 022306 (2016).
[47] V. Semenov, A. Zakharova, Y. Maistrenko, and E. Schöll, AIP Conf. Proc. **1738**, 210013 (2016).
[48] F. P. Kemeth, S. W. Haugland, L. Schmidt, I. G. Kevrekidis, and K. Krischer, Chaos **26**, 094815 (2016).
[49] S. Ulonskaa, I. Omelchenko, A. Zakharova, and E. Schöll, Chaos **26**, 094825 (2016).
[50] R. G. Andrzejak, G. Ruzzene, and I. Malvestio, Chaos **27**, 053114 (2017).
[51] B. K. Bera, S. Majhi, D. Ghosh, and M. Perc, EPL **118**, 10001 (2017).
[52] S. Rakshit, B. K. Bera, M. Perc, and D. Ghosh, Sci. Rep. **7**, 2412 (2017).
[53] N. I. Semenova, G. I. Strelkova, V. S. Anishchenko, and A. Zakharova, Chaos **27**, 061102 (2017).
[54] A.-K. Malchow, I. Omelchenko, E. Schöll, and P. Hövel, Phys. Rev. E **98**, 012217 (2018).
[55] A. E. Botha and M. R. Kolahchi, Sci. Rep. **8**, 1830 (2018).
[56] I. Omelchenko, O. E. Omel'chenko, A. Zakharova, and E. Schöll, Phys. Rev. E **97**, 012216 (2018).
[57] H.-Y. Xu, G.-L. Wang, L. Huang, and Y.-C. Lai, Phys. Rev. Lett. **120**, 124101 (2018).
[58] N. C. Rattenborg, C. J. Amlaner, and S. L. Lima, Neurosci. Biobehav. Rev. **24**, 817 (2000).
[59] R. Ma, J. Wang, and Z. Liu, Europhys. Lett. **91**, 40006 (2010).
[60] H. Sakaguchi, Phys. Rev. E **73**, 031907 (2006).
[61] S. Olmi, A. Politi, and A. Torcini, Europhys. Lett. **92**, 60007 (2010).
[62] J. M. Davidenko, A. V. Pertsov, R. Salomonsz, W. Baxter, and J. Jalife, Nature **355**, 349 (1992).
[63] I. Omelchenko, A. Provata, J. Hizanidis, E. Schöll, and P. Hövel, Phys. Rev. E **91**, 022917 (2015).
[64] Our simulations have shown that self-adaptive drifting can also take place when a perturbation is applied to a multi-headed chimera. The drifting behavior is qualitatively similar to that of a single-headed chimera, and can be explained by the same mechanism. For example, when a two-headed chimera emerges, a perturbation at, say $x_0$, can lead to a global drift of the chimera in the direction determined by the drift of the *closest* incoherent region towards $x_0$. In general, we find that, associated with a multi-headed chimera, the respective distances between

$x_0$ and the middle points of all the incoherent regions are key to determining the drifting direction and velocity.

[65] E. Ott and T. M. Antonsen, Chaos **18**, 037113 (2008).
[66] E. Ott and T. M. Antonsen, Chaos **19**, 023117 (2009).